




Facile fabrication and optical properties of polymer waveguides with smooth surface for board-level optical interconnects

Xiao-Feng Liu^{1,2} , Rui Wang¹, Guo-Dong Wang¹, Teng-Feng Yao¹, Hua Miao^{1,*}, and Rong Sun^{2,*}

¹Shennan Circuits Co.,Ltd., Gao Qiao Industrial Park East, Long Gang District, Shenzhen 518117, China

²Center for Advanced Materials Shenzhen Institutes of Advanced Technology, Chinese Academy of Sciences, Shenzhen 518055, China

Received: 26 July 2022

Accepted: 6 October 2022

Published online:

1 November 2022

© The Author(s), under exclusive licence to Springer Science+Business Media, LLC, part of Springer Nature 2022

ABSTRACT

Polymer waveguides fabricated via conventional lithography or imprinting method usually have step refractive index (SI) cores. For these SI-type polymer waveguides, the surface roughness, especially sidewall roughness may induce rough-interface scattering loss, which is one of the main contributions to the signal attenuation. In this work, on the basis of imprinting method, a novel fabrication method combining thermal reflow process was developed to prepare highly desired optical polymer waveguides. The basic shapes and sizes of pre-fabricated waveguides were conveniently defined by an elastomer stamp with reverse structures of final waveguide link network. The elastomer stamp used for imprinting was fabricated by duplicating the morphology of an initial master following standard replica molding protocols. Then the pre-fabricated waveguides were treated with a low-temperature thermal reflow process to improve the surface quality via the interaction of surface tension and internal stress. The influence of processing parameters on the profiles of the resultant polymer waveguides was systematically investigated and the mode-of-action of thermal reflow process was also proposed. Finally, the optical transmittance properties, including the transmission loss and inter-channel crosstalk of the obtained polymer were investigated, and the corresponding results were carefully discussed. Owing to the decreasing scattering loss induced by surface roughness and the finely-tuned geometry, the as-fabricated waveguides exhibited better optical performance than those of polymer waveguides fabricated via photolithography. Compared with waveguides obtained by conventional photolithography, the resultant multimode optical polymer waveguides with three-dimensional smooth surface exhibited essentially lower propagation loss (0.28 dB/cm) and inter-channel crosstalk (< -30 dB). This work presented here offers new insights for developing polymer waveguides with high surface

Address correspondence to E-mail: Miaoh@scc.com.cn; rong.sun@siat.ac.cn

quality and good optical performance for board-level optical interconnects by a facile and cost-effective approach.

1 Introduction

Owing to inherent disadvantages, including, electromagnetic interference, power consumption, and heat dissipation issues at high operating frequencies and high data rates (> 10 Gb/s), the traditional metal wiring-based electronic interconnect links have almost reached to their functional limits, particularly in ultra-large-scale high-performance electronic systems, such as data centers and supercomputers [1–5]. Optical interconnect technologies have unique characteristics of high density, wide bandwidth, reduced power consumption as well as immunity to electromagnetic interference [6, 7]. Furthermore, they can overcome the shortage of thermal management of electrical interconnect technologies. Accordingly, conventional copper wire has been gradually replaced by optical transmission medium in various link systems, in particular multimode optical fiber (MMF) links, which have been extensively deployed in rack-to-rack communications on account of their low cost, large bandwidth, and convenient assembly [5, 8]. However, in terms of board-level communication, optical interconnect technologies should be compatible with existing electronic system architectures and conventional manufacturing processes of the electronics industry, at the same time allow systems assembly and packaging at low costs [9]. Unfortunately, the drawbacks of optical fiber, like fragile, which is sensitive to temperature and vibration, make the cost-effective integration of optical fiber into existing electronic systems become an intractable technological challenge [10].

Polymer optical waveguides are attractive transmission medium for hybrid integration of photonic devices or chips in on-board optical interconnection networks, owing to their flexible wiring capability and cost-effective integration ability [11–15]. Among various polymer optical waveguides, multimode polymer waveguides have been drawing much attention for potential industrial applications, owing to their large dimensions which can offer relaxed alignment tolerances to enable cost-effective assembly and packaging of systems [16, 17]. Plenty of fabrication technologies, such as optical lithography

[18, 19], imprinting [20, 21], and laser direct writing [22, 23], etc., are introduced to fabricate multimode optical waveguides with polymeric materials. These traditional fabrication technologies provide efficient ways for rapid fabrication of polymer waveguides. However, they all lack the flexibility in fabricating polymer waveguide with appropriate features for achieving low coupling loss with standard optical fibers. Usually, those resultant polymer optical waveguides have typical step refractive index (SI) profiles, for which the attenuation loss is very sensitive to the roughness of the sidewalls. For SI polymer waveguides, optical signals propagate with total internal reflection. In that case, the rough core-cladding boundary of waveguides may cause remarkable scattering effect. Besides, the rough sidewall may lead to the unwanted coupling among guided modes and radiation modes, especially in the case of narrow inter-channel pitches [24]. Clearly, the implementation strategy of low roughness is critical for fabricating waveguides with minimal optical attenuation and less inter-channel crosstalk.

With the advantages of low cost, easy handling, and high-throughput production possibilities, imprinting is considered as one of the most promising alternative techniques for polymer-based micro-nanostructure manufacturing [17, 25]. In terms of polymer waveguides fabrication, the superiorities of imprinting over other techniques are related to their efficiency and cost-effectiveness processes, two-dimensional planar structure, as well as the ability to adjust physical property of the corresponding waveguides. It is obvious that surface quality of related waveguides fabricated by imprinting method is seriously affected by initial master. And surface roughness exerts tremendous negative influences on optical transmission performances of the waveguides [26]. Therefore, ultra-precision imprinting masters (such as silicon/quartz wafer or metallic) are required to fabricate polymer waveguides with fine optical performance [27]. However, these hard and high-quality masters are difficult to be handled, and exhibiting poor compatibility with the existing standard printed circuit boards (PCBs) process flow-charts. Although the roughness of waveguide

sidewall can be minimized by using high-quality masks or some other complex optimized imprinting technologies, there have been comparatively few studies on the application of new flexible method to fine-tune the geometry features of polymer waveguides with high precision while without the use of ultra-precision mold. These advanced methods often require multiple steps and complicated procedures, which might further compromise the pattern fidelity.

Thermal reflow technique is a flexible and mature established post-processing method for fabricating spherical or cylindrical micro-nanostructure with smooth surface [28–30]. During thermal reflow, melting and mass transfer of the structures made by pre-process occur to modify the shape of a binary (i.e., one-level) structure into a three-dimensional (3D) shape. When the temperature is over glass transition temperature T_g , the material changes into a viscous state and surface tension leads to collapsing and the formation of a surface of least energy (surface of minimum area). [31] Thus, the shape of structure is driven to form a spherical or cylinder profile to minimize surface tension. And the final profile depends on the surface critical angle between the substrate and the material. Besides, the thermal reflow process has also been used for the fabrication of micro-nanostructure with reduced sidewall roughness and removal of fabrication defects and deviations in shape from the intended design [32].

Herein, in order to enlarge the scope and flexibility of the portfolio of imprinting and reflow even further and to minimize optical scattering loss caused by sidewall roughness, we developed a new strategy that combined of the imprinting technology and thermal reflow process. Here, lithographically defined resist patterns were used for replica molding of elastomer stamps. Waveguide array with good fidelity in imprinting process was obtained due to thermoplastic nature of the commercially available epoxy-based waveguide materials. The waveguides were then treated with a thermal reflow process to achieve smoother surface and more appropriate contour profile. The cross-section profiles and surface roughness of the polymer waveguides were thoroughly measured. Besides, the corresponding mechanism of the combination strategy on smoothing microstructures was also clarified. This innovative work provides the theoretical and technical guidance for the practical applications of the novel fabrication technologies in mass production of high-quality

optical element with accuracy profile and low roughness.

2 Experimental setup

2.1 Fabrication of master

An initial polymer-based master was lithographically defined by using SU-8 series, a negative-type photoresist purchased from Cchip Co. Ltd (Suzhou, China). The steps involved in the fabrication of reusable SU-8 masters with desired patterns mainly include spray coating and photolithography, which are standard processes employed in PCB manufacturing. Surface roughness of under-cladding layer is strongly dependent on the surface quality of the substrate. Thus a piece of glass with roughness of 12 nm was applied as the substrate. Oxygen plasma was applied to improve adhesion between the polymer and the substrate. A SU-8 wet film with the required solid-state thickness of 50 μm was spray-coated onto the cleaned glass substrate and followed by baking and UV irradiation to form grooves with width of 50 μm and pitch of 250 μm . Hard baking was finally applied to fully cure the master.

2.2 Fabrication of soft mold

Polydimethylsiloxane (PDMS) is easy to handle and demoulding. And it can provide good contact with the substrate than hard molds. These features make PDMS become optimal material for serving as a soft mold in imprinting method. The flexible PDMS mold applied for imprinting was replicated from the fabricated SU-8 master by a cast-molding method and the process is illustrated in Fig. 1. Specifically, the PDMS base (SYLGARD 184, Dow Corning) and the curing agent was mixed to a ratio of 10:1 and the homogeneous mixture of PDMS precursor was stirred and evacuated for about 5 min in a vacuum oven to eliminate bubbles. After vacuum degassing, the mixture was then immediately cast against the SU-8 master. Then, a glass was placed onto the wet film and 2-mm-thick spacers were set between the glass and the master for defining uniform thickness of PDMS soft mold. Subsequently, the whole structure was horizontally put onto a flat plate to avoid the overflow of PDMS precursor. Next, the PDMS mold was cured at room temperature for 48 h and then

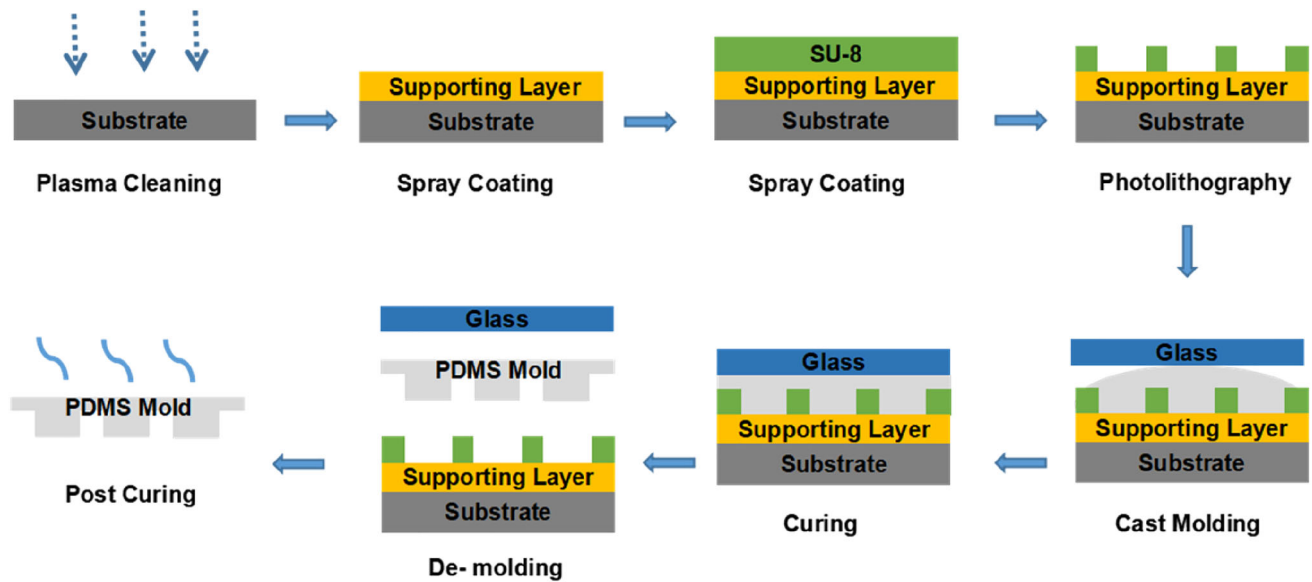


Fig. 1 Schematic representation of process for PDMS soft mold

peeled off from the SU-8 master. It was noteworthy that the stripping direction must be consistent with that of parallel waveguides to avoid physical damage, which would affect the replication quality to a large extent. Finally, the mold was baked at an oven at 150 °C for 30 min to improve the mechanical properties.

2.3 Fabrication of optical waveguides

The commercially available thermal- and UV-curable epoxy resins (EpoClad and EpoCore), supplied by Micro Resist Technology GmbH, Germany, are widely served as cladding and core materials for optical applications. These epoxy-based waveguide materials possess high optical transparency at the wavelength of 850 nm. And their refractive indices at 850 nm are 1.571 and 1.582, respectively. The unexposed EpoCore dry film has a low T_g , and relatively low viscosity above T_g , thus, making it well suited for imprinting technology. Taking advantage of flexible curing process of the UV- and thermal-curable monomers (EpoClad and EpoCore), the preparation of waveguides was tailored into two major convenient processes: imprinting and thermal reflow. Firstly, an EpoClad monomer layer with a wet thickness of approximately 50 μm was spray-coated onto a non-copper-clad FR-4 substrate by plasma-enhanced chemical vapor deposition, and it was acted as the under-cladding layer of waveguide. Then, the film was relaxed for 2 h and then soft-

baked at an oven at 80 °C for 30 min and 120 °C for 60 min. A $\sim 40 \mu\text{m}$ thickness of under-cladding dry film layer was formed so as to ensure optical isolation between the waveguide mode and the underlying substrate. After that, the under-cladding layer was exposed for about 30 s under UV light irradiation by an ultra-high-pressure mercury lamp (UHL, FIC-a5000SG, YUMEX Co., Japan) with a peak emission at 365 nm and irradiance of 40 mW/cm^2 so as to form the three-dimensional cross-linking networks. Subsequently, the film underwent post-baking and hard baking.

For typical imprinting process, the patterned elastomeric mold is placed onto a thin layer of liquid either in melt or in solution state. The capillary force and external pressure drive the spontaneous filling of liquid into the grooves of the patterned mold, replicating the mold morphology when the liquid became solidified upon cooling or UV crosslinking. Clearly, for imprinting method, depending on the available volume of the liquid film relative to the groove volume of the mold, two scenarios, namely, over-filling or incomplete filling might occur. In order to faithfully fabricate imprinted polymer waveguide microstructures, a dry film of EpoCore with a thickness approach to 40 μm was precisely estimated and cast against the as-prepared under-cladding layer. Then, followed by a soft-baking process, which was a crucial step to balance the capability of imprinting-molding and maintaining the relief patterns after de-

molding. The solvent concentration remained in EpoCore film was reduced by evaporation, yet the film became solidified but still sensitive to UV radiation. After lots of trial, the best soft-baking conditions were 50 °C for 30 min and 90 °C for 30 min. Next, the core layer film was then cooled down slowly to the room temperature. And then the PDMS mold was pressed onto the solidified film layer against substrate. A vacuum-assisted molding process was conducted to avoid trapped air bubbles. During the process, the whole structure was heated to the defined temperature. And a pressure of ~ 10 kgf was applied to a glass cover to ensure the viscous flow state of EpoCore monomers were sufficiently squeezed to fill the grooves in PDMS mold. The applied adequate pressure was to ensure compact lamination between PDMS mold and so as to lead to the clearly defined rectangular cores. After maintaining at a defined time, the structure was then natural cooling to the room temperature. After the pressure was released, the PDMS mold was peeled off from the substrate carefully. No obvious air bubbles were observed, which mean that the flexible mold was tightly bonded to the core layer.

After the waveguides were patterned on the substrate, a low-temperature thermal reflow process was conducted at a pre-heated oven. The control factors of thermal reflow process were optimized to realize desired waveguide morphology, which were well discussed in the following section. The waveguides were immediately transferred onto an aluminum heat sink held at room temperature to minimize dwelling time at intermediate temperatures. Subsequently, UV exposure with 1000 mJ/cm^2 was performed to solidify the pre-formed microstructures. After completing core patterns of the waveguides, a sufficient amount of EpoClad monomers were covering on the waveguide patterns to completely fill the grooves and form upper-cladding layer with a thickness of $\sim 60 \mu\text{m}$. Finally, the multimode optical waveguides were successfully fabricated. The steps in the fabrication of multimode polymer waveguides by the combination technique are shown in Fig. 2.

3 Results and discussion

3.1 Morphology of optical waveguide

The micro-morphologies of the SU-8 master and the corresponding PDMS mold were systematically investigated, and the results are shown in Fig. 3. Clearly, the patterns of PDMS soft mold showed in Fig. 3b1 were almost complementary with those of SU-8 master as shown in Fig. 3a1. The patterns in SU-8 master were concave, corresponding to that the patterns in the soft PBDPS mold were convex. The cross-sectional profiles that grooves the PDMS mold had a typical depth of $50 \mu\text{m}$ and a width of $53 \mu\text{m}$, which was slightly higher than that of the master (typically, $51 \mu\text{m}$), ascribing to the expansion of PDMS. As expected, the SU-8 cores had a smooth surface and a vertical but rough sidewall (see Fig. 3a2). The sidewall roughness of the SU-8 master measured by three-dimensional confocal microscope was about 212 nm . And the PDMS mold had a similar sidewall roughness value, which was 206 nm , indicating high replication precision for the cast-molding method.

To obtain the desired shape and suitable profile, the reflow time and temperature often need to be precisely controlled in the traditional thermal reflow process. Thus, the pivotal factors including imprinting temperature and holding time were carefully controlled so as to fabricate the waveguide patterns with high geometric shape quality. A sufficient imprinting pressure of ~ 10 kgf was selected to sustain the viscous flowing state of polymer for filling the grooves completely. Figure 4a and b showed the effects of varied imprinting temperature and holding time on the cross-sectional profile morphologies of polymer trenches. Under $100 \text{ }^\circ\text{C}$, the rectangular geometric profile of waveguide became more obvious with increasing holding time. When the holding time reached to 20 min, the core patterns realized nearly conformal patterns replication of master, as shown in Fig. 4a. The geometry of polymer waveguides tended to be stable when imprinting temperature exceeded $100 \text{ }^\circ\text{C}$. Moreover, regardless of small change in the core size, there were no observable changes in the morphology of imprinted waveguides, when the imprinting time exceeded 15 min as shown in Fig. 4b. The optimum imprinting temperature and holding time, which were typically $100 \text{ }^\circ\text{C}$ and 20 min, respectively, were chosen by considerations of the

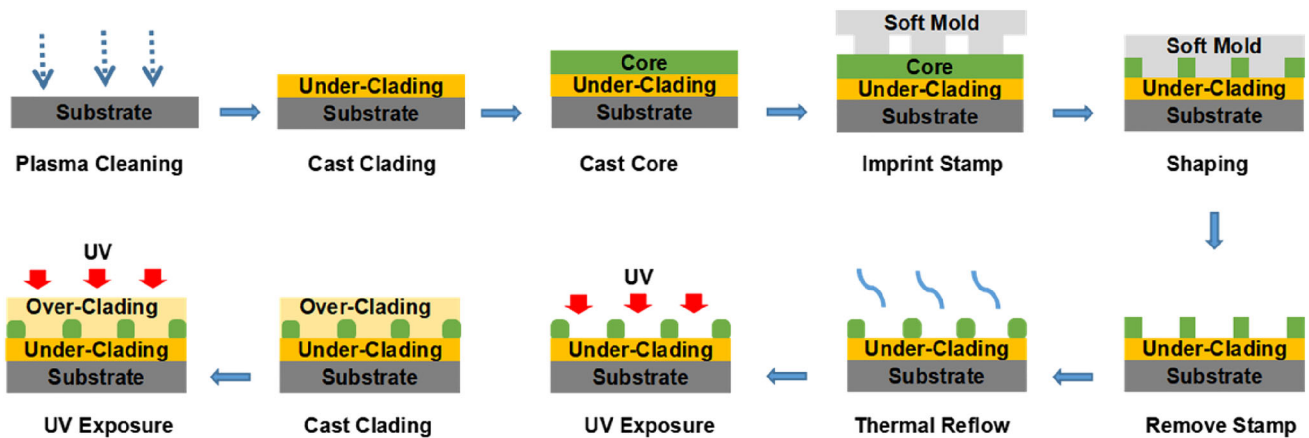


Fig. 2 Schematic representation of process for fabricating embossed polymer optical waveguides with high surface quality

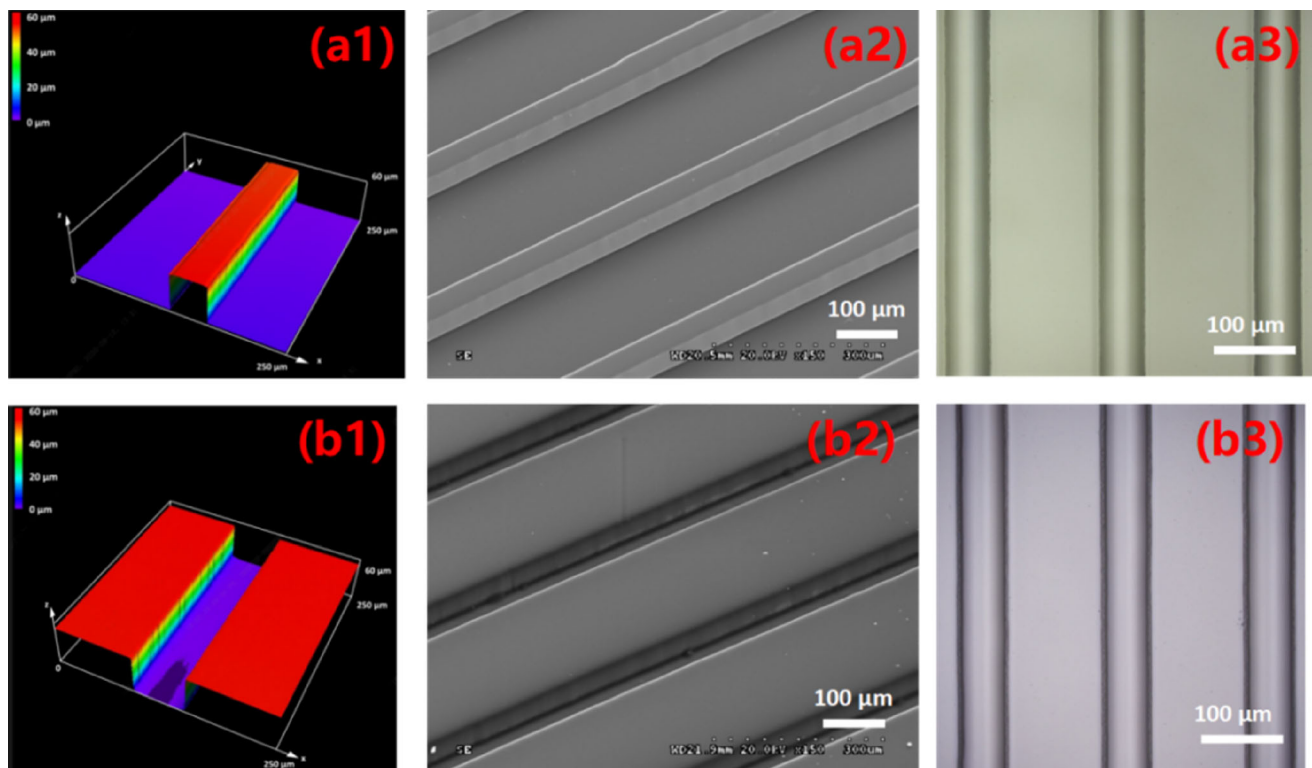


Fig. 3 Typical micro-morphology of SU-8 master and the corresponding PDMS mold: three-dimensional view recorded by three-dimensional laser-scanning confocal microscopy (a1 and

b1), SEM images and (a2 and b2) optical microscope images (a3 and b3), respectively

viscous behavior of the imprinted polymer, the superiority in rapid mass transport, homogeneous pattern transfer, and minimized thickness of residual layer. The representative SEM images of imprinted polymer waveguides are shown in Fig. 4c. The desired rectangular shape of waveguide with an average core size of approximately $50 \times 50 \mu\text{m}$ was basically formed. And all the fabricated waveguides

had a uniform square shape with consistent dimensionality (see Fig. 4c1 and c2). The geometric dimensions of replicated waveguides were also measured by optical microscopy and the results were found to be in good agreement with that of the profilometer measurements. It is noted that the slight difference in heights of the polymer waveguide arrays as shown in Fig. 4c2 was probably related to

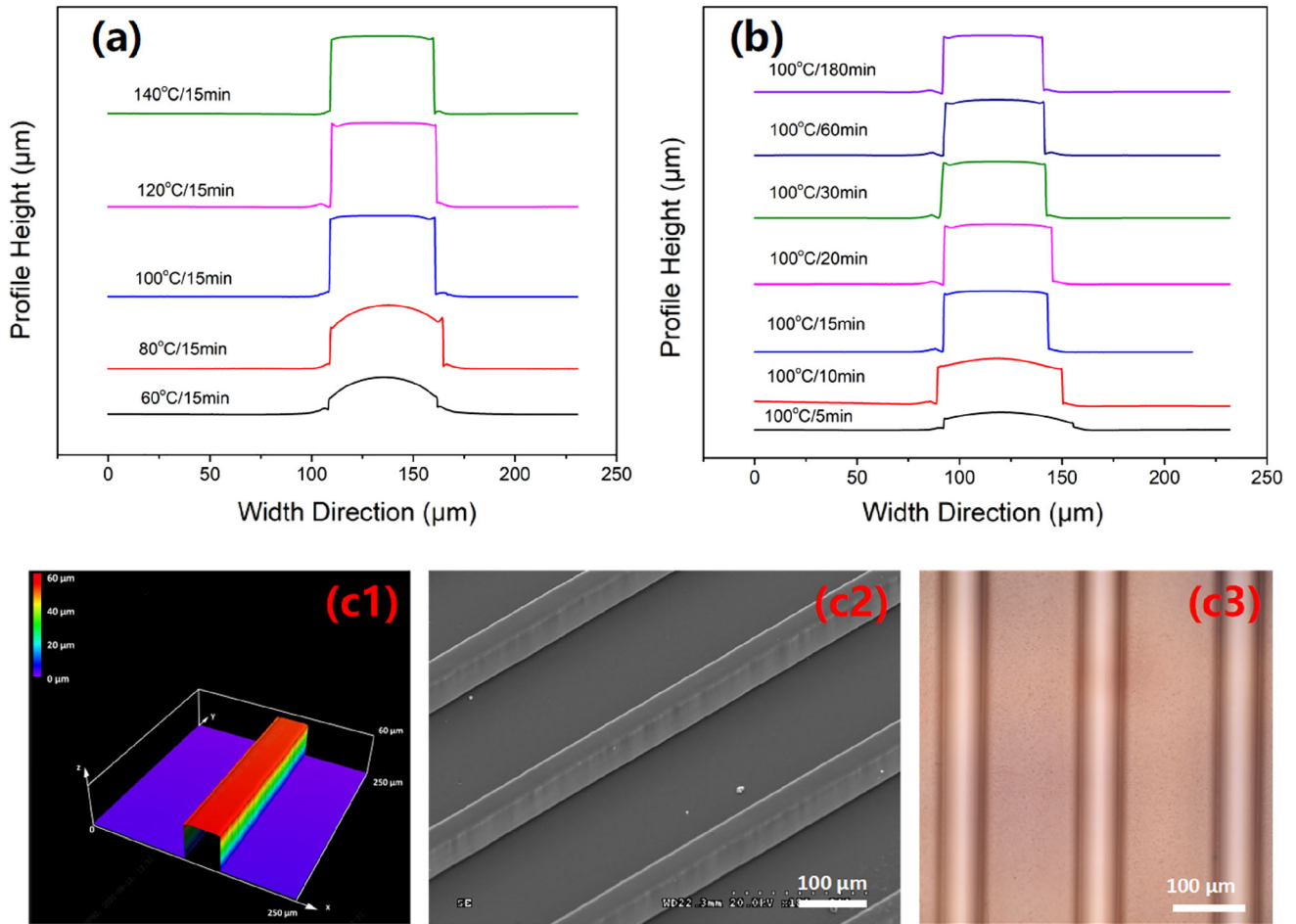


Fig. 4 Cross-sectional profiles of the fabricated polymer waveguides under different imprinting temperatures at a fixed holding time of 20 min (a). Profiles of waveguides at cross section under different holding times at a fixed temperature of 100 °C (b).

Three-dimensional view (c1), SEM images (c2), and optical microscope images (c3) of the replicated polymer waveguides, respectively

the uniform imprinting force. The aforementioned results indicated that the overall waveguide patterns were precisely transferred without any shape distortion.

Thermal reflow process has been widely employed as smoothening method to produce ultra-smooth optical micro-nanostructures. Nevertheless, un-controlled thermal reflow is undesirable, which might lead to the deterioration of structural integrity of the desired patterns. Here, in order to optimize annealing temperature to prevent the waveguide arrays from crawling during thermal reflow process, the annealing temperature was close around the melt temperature of the solidified EpoCore. Cross-sectional profiles of the resultant waveguides those were thermal treated at different temperature were precisely compared. As shown in Fig. 5a, with increasing

the thermal reflow temperature, the swallowtail deformation was significantly alleviated in the edge profiles of waveguide trenches due to enhanced polymer viscous flowing property. Well-defined shape of waveguide arrays were obtained at 55 °C. However, once the reflow temperature reached or exceeded 60 °C, the patterns collapse occurred and obvious defects appeared on the surface of waveguide. The comparisons of cross-section profiles of polymer waveguides treated at different thermal reflow time were measured and the corresponding results are shown in Fig. 5b. The profilometer measurements were conducted to further investigate the variation of height and width of polymer waveguides, and the results are shown in Fig. 5c. After the thermal reflow process, the shape of waveguides was transformed from rectangle structure to cylindrical

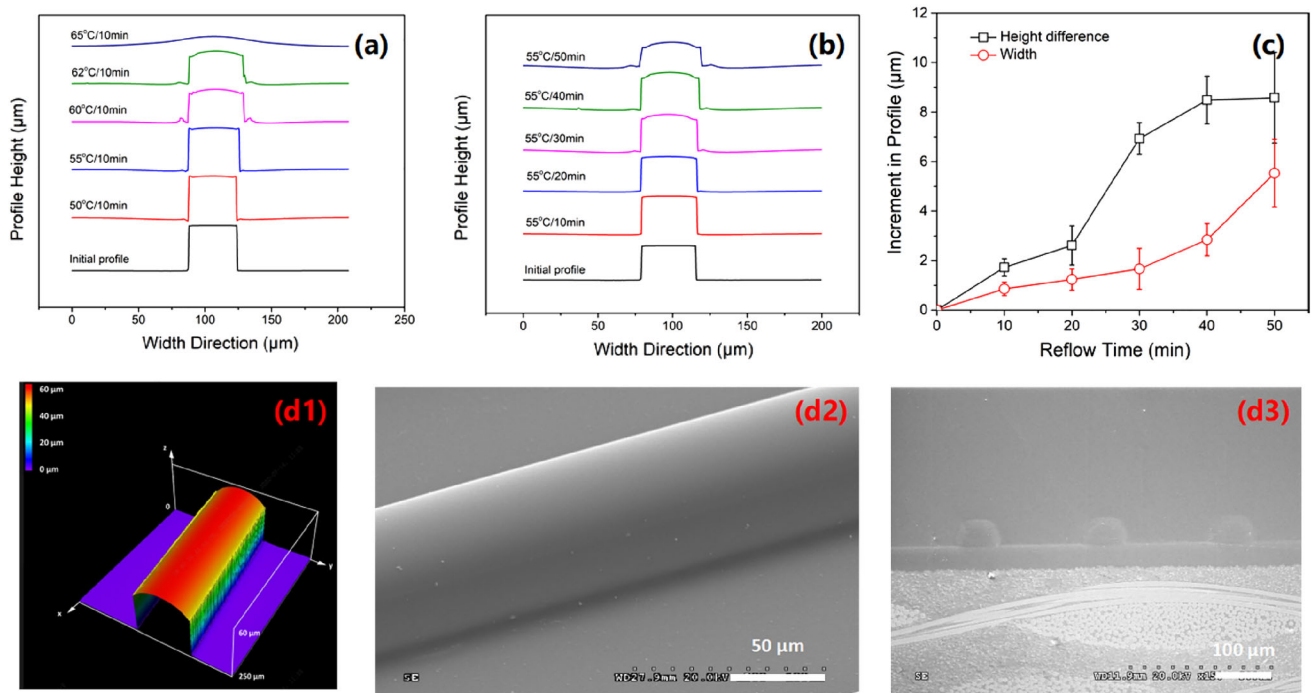


Fig. 5 Cross-sectional profiles of the related polymer waveguides under different reflow temperatures at a fixed reflow time of 10 min (a) and under different reflow times at a fixed reflow temperature of 55 °C (b). The increment in the profile of waveguides as the increasing reflow time (c). Three-dimensional

structure by the surface tension effect in the molten state. Optical microscopy was also applied to measure the width and height difference of the replicated waveguides and the results were consistent with those of the profilometer measurements. Clearly, the height difference of the embossed waveguides was regularly increased as the increasing thermal reflow. It rapidly increased initially as the reflow time rose, and then leveled off when the reflow time approached to 30 min (Fig. 5c). The height difference was defined as the height difference from the top of the waveguide ridge to the baseline, see Fig. 7a. After the reflow time reached 50 min, the collapse of waveguide occurred. The total height of waveguide sharply decreased to 35 μm, and obvious expansion in width direction appeared. After the thermal reflow of 40 min, the width of waveguide core had a typical value of 51 μm with a variation of 5 μm, and the height was on a typical value of 55 μm with a variation of 3 μm. The slight changes in the size of waveguides can be explained by the relaxation and expansion of the waveguides during the thermal reflow processing, which will be discussed in the following sections. The pre-modeled shape profiles

view of the fabricated polymer waveguide after thermal reflow (d1). SEM images of polymer waveguide: typical oblique view with a period of 50 μm (d2); typical cross-sectional micrograph (d3)

remained almost unchanged even if the reflow time extended 20 min. However, once the thermal reflow time exceeded 40 min, waveguide patterns collapse occurred, as evidenced by the horizontally extended profiles of waveguides (see Fig. 5b). These results indicated that this feature can be utilized for fabricating optical waveguide with low roughness and cylinder-shaped structure by a precise control of the polymer reflow process.

The three-dimensional images of resultant multi-mode optical waveguides after thermal reflow treatment further confirmed their nature of curvature and surface smoothness. (Fig. 5d1). SEM was applied to characterize the cross-section morphology of the as-fabricated waveguide and the results are displayed in Fig. 5d2 and d3. The initial waveguides were orderly arranged and the edges of waveguides were fairly clear (see Fig. 4c). Remarkably, the entire surface of waveguide was quite smooth after thermal reflow. Besides, the sharp corner of sidewall edge disappeared and the profile was approximate to be a spherical profile, see Fig. 5d2. The spherical geometric shape of waveguide core might provide higher coupling efficiency with MMFs than that of

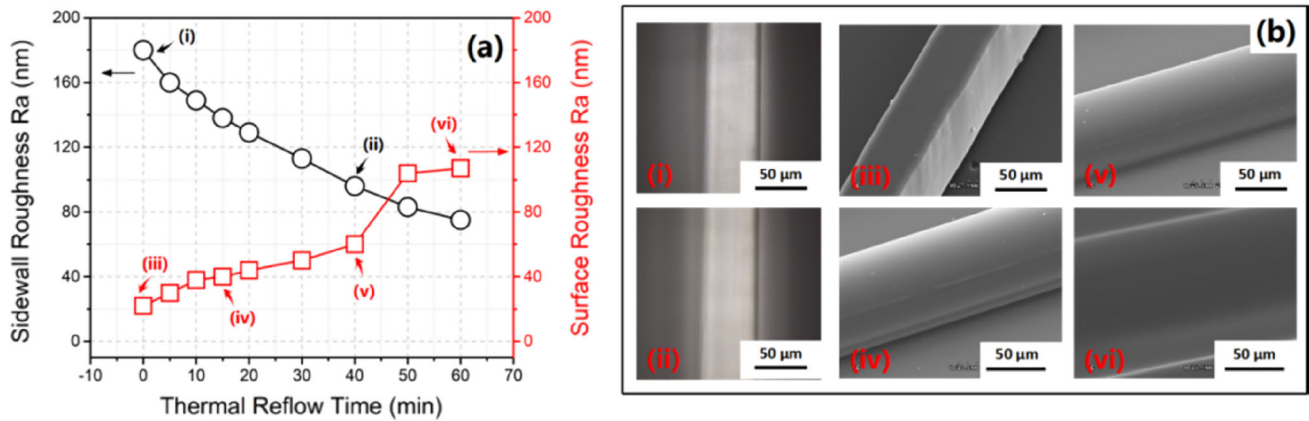


Fig. 6 Sidewall and surface roughness of the fabricated optical waveguide varied with thermal reflow time (a). Typical representative SEM images of the waveguides at different stages during the thermal reflow process (b): sidewall of the initial

waveguide (i), sidewall of the waveguide after reflow 40 min (ii), initial waveguide (iii), after reflow 20 min (iv), after reflow 40 min (v), and after reflow 60 min (iv), respectively

rectangular waveguide because the homologous core structure offers better mode-field matching no matter in size or shape. The residual layer of waveguide core is a common problem in the soft imprinting process, which may lead to large optical power loss and serious channel crosstalk. In this work, the amount of residual layer was related to the initial film thickness of EpoCore and the soft-baking process. It was worth to note that the processing parameters were optimized to obtain the minimized residue layer. As shown in Fig. 5d3, a residual layer with average thickness of less than 5 μm for core material was observed.

In order to systematically study the effect of thermal reflow process on the roughness of resultant waveguides, the surface and sidewall roughness of waveguides after thermal reflow treatment at 55 °C were evaluated by means of a three-dimensional laser-scanning confocal microscopy and the results are shown in Fig. 6a. As a representative for embossed waveguides fabricated via the soft imprinting method, the average surface roughness (R_a) of the related waveguides was ~ 20 nm, while the sidewall roughness was ~ 182 nm, which arose from the initial SU-8 master. However, the surface quality of waveguides after the low-temperature thermal reflow process significantly improved, of which the sidewall roughness was drastically decreased from 182 to 83 nm, accompanying by a slight increment in surface roughness. Obviously, the waveguides experienced subsequently sharply increase in surface roughness once the reflow time exceeded 40 min due

to the effusion of waveguides. These results indicated that high-quality multimode polymer waveguide with cylinder shape and three-dimensional smooth surface was successfully prepared.

3.2 Mechanism of thermal reflow

Mechanism of the thermal reflow process on smoothing microstructures was also clarified. In broad terms, the volume of micro-nanostructure before and after reflow is usually assumed to be the same. For a columnar structure, its volume is equal to the length times the area of cross section. Figure 7a shows the model of the cross section before and after reflow. In this model, the waveguide is divided into two regions, namely, the deformation generation region (in green) and the deformation retention region (in shadow). During the thermal reflow process, the length of structure basically remains unchanged, which means that the area of deformation generation region remains unchanged before and after the reflow process. Before the reflow, the cross-section area (S_A) is determined by the upper width d_0 , the lower width d_1 , the height h_1 , and side wall angle α .

$$S_A = \frac{(d_0+d_1) * h_1}{2} = (d_1 - h_1 \cot\alpha) * h_1 \tag{1}$$

After the reflow, the cross section can be regarded as a circle arc with a certain curvature and its area (S_B) is determined by the curvature radius R , the cylindrical waveguide width d_2 , and height h_2 :

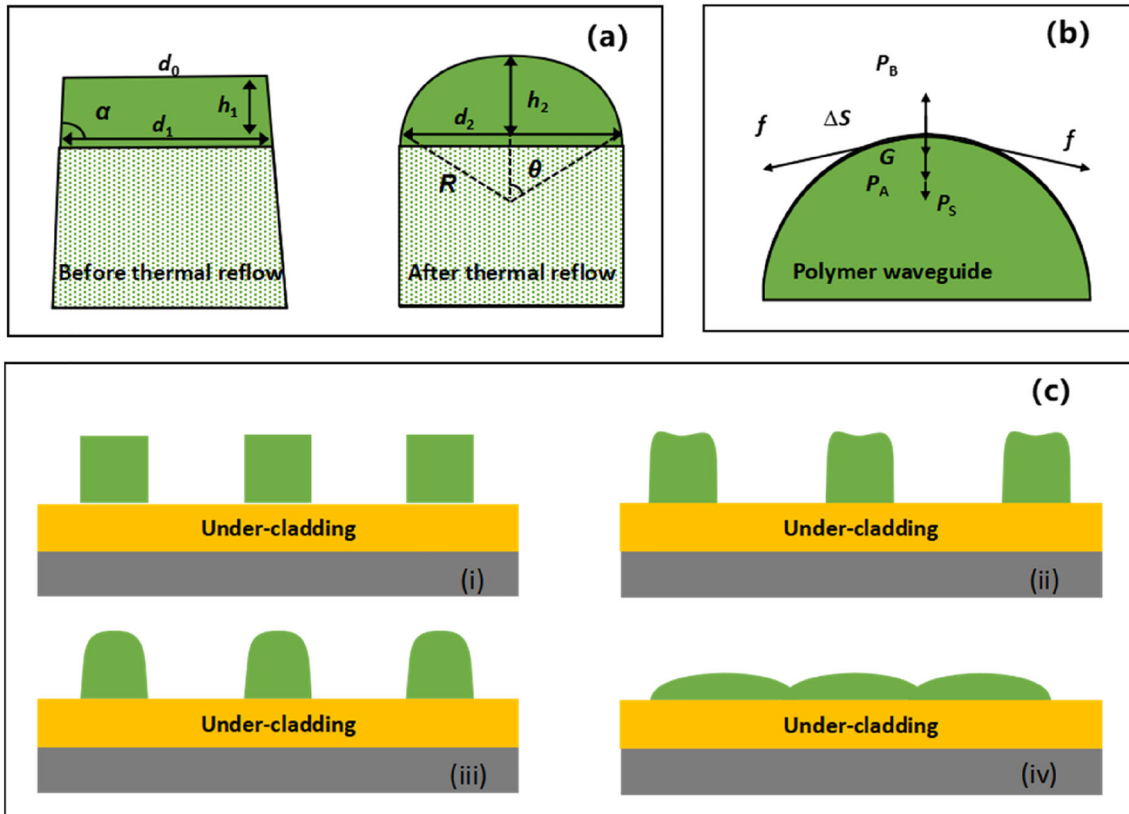


Fig. 7 (a) Mathematical model of the cross section before and after reflow. (b) Model of mechanical analysis for the thermal reflow. (c) Schematic of morphologies of waveguides at different

stages during the reflow process: initial stage (i); shape corners smooth stage (ii); rise stage (iii); collapse stage (iv)

$$S_B = R^2 * \arcsin \frac{d_2}{2R} - \frac{d_2 * \sqrt{R^2 - d_1^2/4}}{2} \tag{2}$$

In this work, the upper width d_0 and the lower width d_1 can be regarded as the same. The sidewall angle α is about 90° . And the width had a variation of $3 \mu\text{m}$, before and after the thermal reflow, which was small enough to be ignored, when compared with the height, which meant that the value of d_2 was close to d_1 . In this case, the formula can be simplified as

$$d_1 * h_1 = R^2 * \arcsin \frac{d_1}{2R} - \frac{d_1 * \sqrt{R^2 - d_1^2/4}}{2} \tag{3}$$

Here, the width (d_1) of waveguides was about $51 \mu\text{m}$. The height (h_1) of waveguides was about $8 \mu\text{m}$ with a variation of $2 \mu\text{m}$. Thus, the curvature radius R changed from 41.4 to $30.0 \mu\text{m}$, which indicated that the repeatability of the waveguides could be obtained to a certain extent. The EpoCore monomers can be regarded as pseudo-plastic fluid after partial thermal cured, of which the Deborah number is far smaller

than 1. In that case, the flow can be assumed to be Newtonian with constant viscosity during the low-temperature thermal reflow process, and the reflow process can be described by the Navier–Stokes equation [33]. For the Navier–Stokes equation,

$$\rho \left(\frac{\partial v}{\partial t} + v \cdot \nabla v \right) = -\nabla p + \eta \nabla^2 v + \rho g, \tag{4}$$

where ρ is the density, v is a speed vector, η is the viscosity, p is the pressure, and g is the gravitational acceleration. Owing to the fact that the monomers have a high viscosity and there are no shear force involved in the thermal reflow, the Reynolds number for the static reflow process is much smaller than 1. In that case, the left side of (1) can be equal to zero, and the creep flow model can be described as the following simplified equation:

$$-\nabla p + \eta \nabla^2 v + \rho g = 0. \tag{5}$$

The typical values of p , η , and ρ for optical waveguide resins are $0.02\text{--}0.05 \text{ N/m}$,

2000–10,000 mPa s, and 1.1–1.3 g/cm³, respectively [34]. In this work, the typical features of polymer waveguides are 50 μm. According to the simplified equation, at the given submicron geometrical scale and for highly viscous fluids, gravitational effect can be omitted and surface tension plays the critical role during the reflow process [35]. According to the basic mechanical analysis as shown in Fig. 7b, an equilibrium equation is in the vertical direction, $P_B = P_A + P_S$ for a microunit ΔS of molten polymer waveguide profile surface, where P_B , P_A , P_S are internal pressure, atmospheric pressure, and additional force caused by surface tension, respectively. The internal pressure P_B is positively related to the thickness. When the temperature approaches to or above T_g , it always has $(P_B = P_A + P_S) > P_A$, which indicates that the profile height will increase with the reflow time extending [36], and finally tends to be stable when $P_B = P_A$. According to the low-temperature thermal reflow strategy, the profile height can be well controlled, while a little deformation of profile will be generated. The analysis results were in accordance with the simulation results in the reported paper [36, 37].

For thermoplastic micro-structured waveguides fabricated by soft imprinting method, pattern relaxation might take place during the thermally treated process. The pattern relaxation can be driven by different driving forces. Schematic of morphologies of waveguides at different stages during the reflow process is presented in Fig. 7c. Firstly, for an ideal reflow process without constraint forces, micro-structured waveguide was triggered by internal stress relaxation. When the temperature increased nearly or above the T_g of polymer matrix, the storage modulus decreased and as a result, a rubber-like elastic recovery occurred. Consequently, the volume expansion of the waveguide occurred and the ridge of the waveguide uplifted, as evidenced by the profilometer measurement results (ii). This phenomenon was particularly significant for semi-cured polymers with high chain entanglement. Subsequently, the polymer entered into the viscous flow state. During this state, the shape of waveguide evolved and tended to be stable with the balance between the surface tension, which tended to smooth the bumps and protrusions, and the viscous sheared, which damped the flow (iii). With the increase of reflow time, surface tension became the primary driving force of pattern decay causing polymer material to slump or reflow,

which ultimately would cause the patterns to retreat and finally flatten onto the surface. That was to say, if the reflow time was further extended, the waveguide would reach a steady state and become completely flat (iv).

3.3 Optical characteristics of polymer waveguides

Prior to optical measurement, the end-facets of the as-prepared 100-mm-long polymer waveguides were polished using mechanical polishing processes by virtue of a specific clamp to obtain smooth and flat end-faces. In order to experimentally demonstrate the superiority of this method, the insertion loss of waveguides fabricated by the same materials via traditional direct-contact lithography technique was also investigated. The experimental setup is shown in Fig. 8a. A distributed feedback laser (DFL, JW-8001, Join Wit Co. Ltd, Shanghai, China) working at 850 nm was used as light source. Matching oil with a refractive index of 1.47 at 1310 nm was applied to both the input and output facets of waveguide to maximally reduce the Fresnel reflection. All 12 channels of the straight waveguides were measured and the results are shown in Fig. 8b. The average insertion loss (including total coupling loss) of the photolithography-type waveguides from Ch. 1 to Ch. 12 was about 3.45 dB. Owing to the smoothness of the core-cladding boundary, the fabricated waveguides exhibited reduced propagation loss. Compared to the conventional counterparts, the average insertion loss (including total coupling loss) of the hot embossed waveguides was about 2.78 dB. In order to elucidate the superiority of the high-quality waveguides, the propagation loss and coupling loss of the related waveguides with MMFs were further determined by cut-back method. As shown in Fig. 8b, the measured propagation loss and coupling loss for waveguides fabricated by the combination method were 0.28 dB/cm and 0.05 dB, respectively, which were lower than those of waveguides obtained by photolithography (0.33 dB/cm and 0.22 dB, respectively). The decreased insertion loss and higher coupling efficiency with MMFs were attributed to the improved interface quality and cylinder geometric form of the fabricated waveguides, which provided stronger confinement effect of optical signal.

The inter-crosstalk of waveguides at 850 nm was measured using the same experimental setup, and

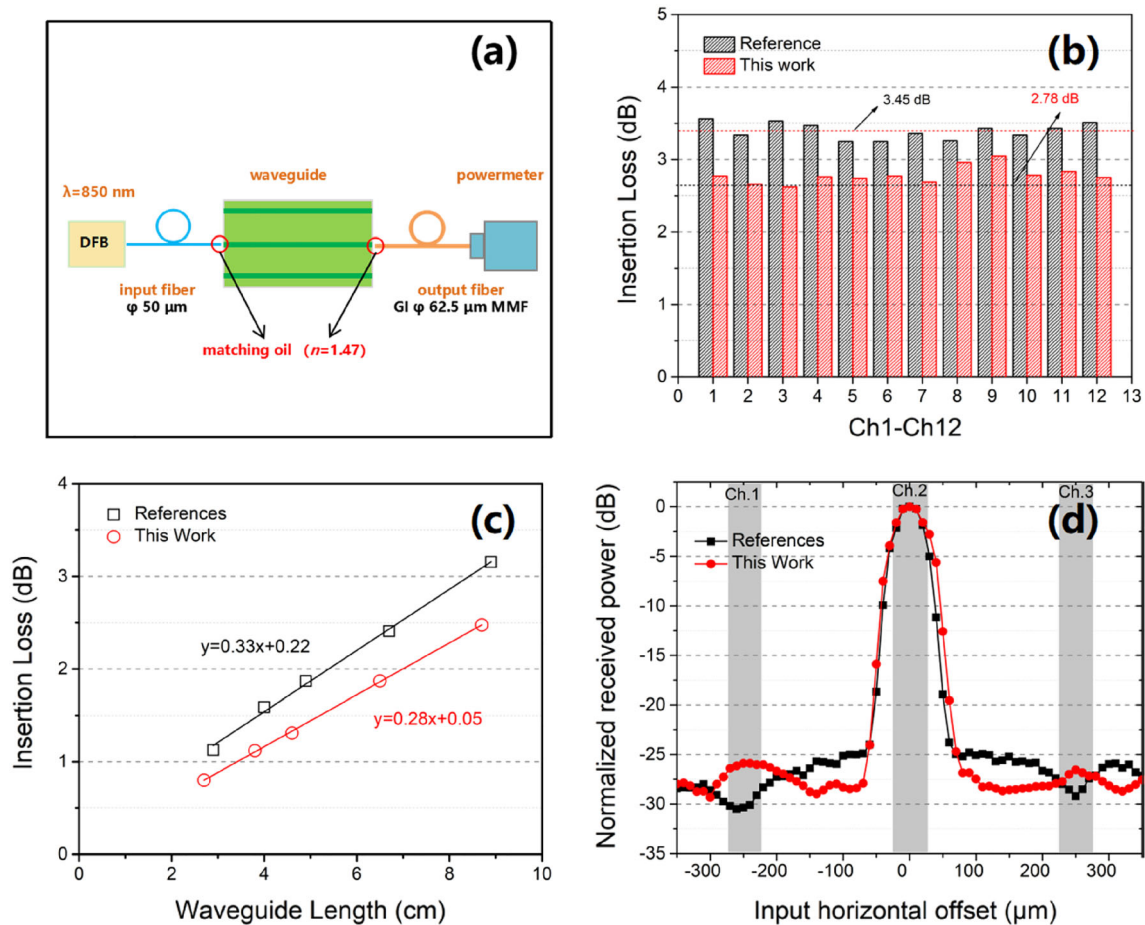


Fig. 8 (a) Schematic of optical characteristics measurements (@850 nm). (b) Measured insertion loss of all 12 channels of 100-mm-long waveguides fabricated by this method and photolithography. (c) Measured propagation loss and coupling

the results are shown in Fig. 8d. By fixing the input fiber and scanning the output fiber in the horizontal direction with a step of 10 μm , the optical power was record at different positions. The light was centrally launched into the Channel 2 (Ch.2) and Channel 3 (Ch.3) from a 50- μm -core GI fiber with matching oil applied on both the input and output ports. Since the straight waveguides had a pitch as large as 250 μm , the inter-channel crosstalk was mainly caused by the mode conversion, which attributed to the coupling of cladding layer scattered light due to imperfections, which majorly arose from the surface roughness of waveguides. The crosstalk results revealed that the maximum inter-channel crosstalk measured at the output port of the adjacent 100-mm-long waveguides was approximately -30 dB (Ch.1 and Ch.3). For comparison, the inter-channel crosstalk of the

loss using a cut-back method. (d) Normalized received power at the output side as a function of the horizontal offset of output fiber. The gray stripes represented the positions of the waveguide cores

waveguides fabricated by photolithography was much higher, -25 dB for Ch.3 and -27 dB for Ch.1. The significant decrease of inter-channel crosstalk in the adjacent channels was ascribed to most of the light signals which were reflected at smooth surface of the core-cladding boundary rather than leaked and directly coupled into the adjacent channels. The optical transmission characteristics of the fabricated waveguides had experimentally demonstrated that the superiority of smooth surface in reducing inter-channel crosstalk and propagation loss, which were very conducive to board-level optical interconnects.

4 Conclusions

High-quality multimode polymer waveguide arrays with tunable geometries were fabricated at the absence of high-precision imprinting mold by combining soft imprinting technique with a low-temperature thermal reflow process. The thermal reflow process was applied to reduce the surface roughness and generate new section geometry of waveguide patterns. Under the interaction of surface tension and internal pressure, the geometry of waveguides was gradually transformed from rectangular to nearly circular during the thermal reflow process. Furthermore, the sidewall roughness of waveguides was drastically decreased from 182 to 83 nm. The measured transmission loss of the as-prepared waveguides at a wavelength of 850 nm was 0.28 dB/cm, corresponding to the coupling loss of 0.05 dB. And a low inter-channel crosstalk (≤ -30 dB) on the output facet in horizontal directions was also achieved. Better optical performance than those of polymer waveguides fabricated via photolithography was ascribed to the decreased scattering loss induced by surface roughness and the finely tuned geometry. The aforementioned results suggest that the proposed facile and cost-effective combination fabrication strategy avoids the lengthy and complexity of fabricating processes, offering great superiorities for mass production of high-quality polymer optical waveguides for photonics and integrated optics applications.

Acknowledgements

Financial supports by the Key R & D Projects of Guangdong Province (Grant No. 2020B010180001). The authors wish to thank Yong-Kai Li of Shennan Circuits Co.,Ltd. for his invaluable contributions to this study. The authors also thank M.S Zhao Yan Zhu, Dr. Yang, and Dr. Chang-Lian Xu for their useful advice and English checking. The authors are grateful for the support of Shenzhen Institute of Advanced Electronic Materials.

Author contributions

The work was done by X-FL and RW under the supervision of HM and G-DW. The manuscript was

written and revised by XFL. All authors have provided helpful suggestions for the experiments. All authors have given approval to the final version of the manuscript. X-FL: Conceptualization, Investigation, Supervision, Writing—original draft, and Writing—review & editing. RW: Investigation, Methodology, and Validation Formal analysis. G-DW: Conceptualization and Supervision. T-FY: Investigation. HM: Resources, Supervision, and Project administration. RS: Conceptualization, and Writing—review & editing.

Data availability

The data underlying this study are available in the article itself.

Declarations

Conflict of interest The authors declare that they have no conflict of interest.

References

1. R. Mahajan, X.Q. Li, J. Fryman et al., Co-packaged photonics for high performance computing: status, challenges and opportunities. *J. Lightwave Technol.* **40**(2), 379–392 (2022)
2. R. Dangel, J. Hofrichter, F. Horst et al., Polymer waveguides for electro-optical integration in data centers and high-performance computers. *Opt. Express* **23**(4), 4736–4750 (2015)
3. M.A. Taubenblatt, Optical Interconnects for high-performance computing. *J. Lightwave Technol.* **30**(4), 448–457 (2012)
4. X.F. Liu, R. Wang, G.D. Wang et al., Fabrication and performance evaluation of flexible polymer waveguides for board-level optical interconnection application. *Acta Optica Sinica* **42**(5), 0523001 (2022)
5. S. Yang, L. Yang, B. Li et al., Fabrication and transmission of optical polymer waveguide backplane for high-performance computers. *Opt. Express* **28**(10), 14605–14617 (2020)
6. R. Zhang, Fuhan et al., Cointegration of Single-mode waveguides and embedded electrical interconnects for high-bandwidth communications. *IEEE Trans. Compon. Packaging Manuf. Technol.* **10**(3), 393–399 (2020)
7. J. Jou, T. Shih, C. Chiu, 400Gb/s optical transmitter and receiver modules for on-board interconnects using polymer waveguide arrays [J]. *OSA Continuum* **1**(2), 658–667 (2018)
8. S. Fathololoumi, D. Hui, S. Jadhav et al., 1.6 Tbps silicon photonics integrated circuit and 800 Gbps photonic engine for

- switch co-packaging demonstration. *J. Lightwave Technol.* **39**(4), 1155–1161 (2020)
9. R.S. John, C.M. Amb, B.W. Swatowski et al., Thermally stable, low loss optical silicones: a key enabler for electro-optical printed circuit boards. *J. Lightwave Technol.* **33**(4), 814–819 (2015)
 10. J.B. Mao, W. Yang, X.J. Feng et al., Research status of flexible electro-optical circuit for interconnection. *Laser Optoelectron. Progress* **53**(8), 080004 (2016)
 11. H. Ma, A.K.Y. Jen, L.R. Dalton, Polymer-based optical waveguides: materials, processing, and devices. *Adv. Mater.* **14**(19), 1339–1365 (2002)
 12. S. Yu, X. Qiu, H. Zuo et al., Compact and fabrication-tolerant waveguide bends based on quadratic reflectors. *J. Lightwave Technol.* **38**(16), 4368–4373 (2020)
 13. S. Nocentini, F. Riboli, M. Burrelli et al., Three-dimensional photonic circuits in rigid and soft polymers tunable by light. *ACS Photonics* **5**(8), 3222–3230 (2018)
 14. X. Zhang, A. Hosseini, X. Lin et al., Polymer-based hybrid-integrated photonic devices for silicon on-chip modulation and board-level optical interconnects. *IEEE J. Sel. Top. Quantum Electron.* **19**(6), 196–210 (2013)
 15. Y. Enami, C.T. Derose, D. Mathine et al., Hybrid polymer/sol-gel waveguide modulators with exceptionally large electro-optic coefficients. *Nat. Photonics* **1**(3), 180–185 (2007)
 16. M. Oh, W. Chu, J. Shin et al., Polymeric optical waveguide devices exploiting special properties of polymer materials. *Opt. Commun.* **362**(362), 3–12 (2016)
 17. M. Jiang, D. Zhang, T. Lian et al., On-chip integrated optical switch based on polymer waveguides. *Opt. Mater.* **97**, 109386.1–109386.6 (2019)
 18. J. Dong, K.S. Chiang, W. Jin, Compact three-dimensional polymer waveguide mode multiplexer. *J. Lightwave Technol.* **33**(22), 4580–4588 (2015)
 19. L. Jin, X. Fu, B. Yang et al., Optical bistability in a high-Q racetrack resonator based on small SU-8 ridge waveguides. *Opt. Lett.* **38**(12), 2134–2136 (2013)
 20. W. Jin, K.S. Chiang, K.P. Lor et al., Industry compatible embossing process for the fabrication of waveguide-embedded optical printed circuit boards. *J. Lightwave Technol.* **31**(24), 4045–4050 (2013)
 21. X.Y. Han, Z.L. Wu, S.C. Yang et al., Recent progress of imprinted polymer photonic waveguide devices and applications. *Polymers* **10**(6), 603 (2018)
 22. Z. Ding, H. Wang, T. Li et al., Fabrication of polymer optical waveguides by digital ultraviolet lithography. *J. Lightwave Technol.* **40**(1), 163–169 (2022)
 23. A. Landowski, D. Zepp, S. Wingerter et al., Direct laser written polymer waveguides with out of plane couplers for optical chips. *APL Photonics* **2**(10), 106102 (2017)
 24. X. Xu, L. Ma, S. Jiang et al., Circular-core single-mode polymer waveguide for high-density and high-speed optical interconnects application at 1550 nm. *Opt. Express* **25**(21), 25689–25696 (2017)
 25. Y.W. Jiang, B.Q. Luo, X. Cheng, Enhanced thermal stability of thermoplastic polymer nanostructures for nanoimprint lithography. *Materials* **12**(3), 545 (2019)
 26. Y. Shi, L. Ma, X. Xu et al., Investigation of roughness induced scattering loss of polymer waveguides for optical printed circuit board application. *OptoElectron. Commun. Conference* (2019). <https://doi.org/10.23919/PS.2019.8817666>
 27. D. Cai, A. Neyer, Polydimethylsiloxane (PDMS) based optical interconnect with copper-clad FR4 substrates [J]. *Sens. Actuators B* **160**(1), 777–783 (2011)
 28. F.T. O'Neill, J.T. Sheridan, Photoresist reflow method of microlens production Part I: background and experiments. *Optik* **113**(9), 391–404 (2002)
 29. J. Zhu, M. Li, J. Qiu et al., Fabrication of high fill-factor aspheric microlens array by dose-modulated lithography and low temperature thermal reflow. *Microsyst. Technol.* **25**(4), 1235–1241 (2019)
 30. M.K. Park, H.J. Lee, J.S. Park et al., Design and fabrication of multi-focusing microlens array with different numerical apertures by using thermal reflow method. *J. Optical Soc. Korea* **18**(1), 71–77 (2014)
 31. H. Schiff, C. Spreu, A. Schleunitz et al., Shape control of polymer reflow structures fabricated by nanoimprint lithography. *Microelectron. Eng.* **88**(1), 87–92 (2011)
 32. Q. Xia, P.F. Murphy, H. Gao et al., Ultrafast and selective reduction of sidewall roughness in silicon waveguides using self-perfection by liquefaction. *Nanotechnology* **20**(34), 345302 (2009)
 33. E. Rognin, S. Landis, L. Davoust, Viscosity measurements of thin polymer films from reflow of spatially modulated nanoimprinted patterns. *Phys. Rev. E* **84**(4), 041805 (2011)
 34. Y. Zhang, C.T. Lin, Y. Shu, Fabrication of hierarchical pillar arrays from thermoplastic and photosensitive SU-8. *Small* **6**(6), 768–775 (2010)
 35. S. Huang, M. Li, L. Shen et al., Fabrication of high quality aspheric microlens array by dose-modulated lithography and surface thermal reflow. *Opt. Laser Technol.* **100**, 298–303 (2018)
 36. J. Qiu, M. Li, H. Ye et al., Fabrication of high fill-factor microlens array using spatially constrained thermal reflow. *Sens. Actuators A* **279**, 17–26 (2018)

37. J. Chao, M. Li, J. Qiu et al., Fabrication of seamless roller mould with smooth surface microstructures by rotation lithography and reflow process. *Micro Nano Letters* **13**(7), 1052–1056 (2018)

Publisher's Note Springer Nature remains neutral with regard to jurisdictional claims in published maps and institutional affiliations.

Springer Nature or its licensor (e.g. a society or other partner) holds exclusive rights to this article under a publishing agreement with the author(s) or other rightsholder(s); author self-archiving of the accepted manuscript version of this article is solely governed by the terms of such publishing agreement and applicable law.